Electrically responsive materials based on polycarbazole/sodium alginate hydrogel blend for soft and flexible actuator application

Watchara Sangwan[a], Karat Petcharoen[a], Nophawan Paradee[a], Wanchai Lerdwijitjarud[b], Anuvat Sirivat[a,*]

[a] The Petroleum and Petrochemical College, Chulalongkorn University, Bangkok 10330, Thailand
[b] Department of Materials Science and Engineering, Faculty of Engineering and Industrial Technology, Silpakorn University, Nakornpathom 73000, Thailand

ARTICLE INFO

ABSTRACT

The electromechanical properties, namely the storage modulus sensitivity and bending, of sodium alginate (SA) hydrogels and polycarbazole/sodium alginate (PCB/SA) hydrogel blends under applied electric field was investigated. The electromechanical properties of the pristine SA were studied under effects of crosslinking types and SA molecular weights, whereas the PCB/SA hydrogel blends were studied under the effect of PCB concentrations. The storage modulus sensitivity and bending of the pristine SA as crosslinked by the ionic crosslinking agent were found to be higher than those of the covalent crosslinking. The storage modulus sensitivity and deflection of the SA increased monotonically with increasing molecular weight. The highest electromechanical response of the PCB/SA hydrogel blends was obtained from the blend with 0.10% v/v PCB as it provided surprisingly the highest ever storage modulus sensitivity, $(G' - G'_0)/G'_0$ where G'_0 and G' are the storage modulus without and with applied electric field, respectively, at 18.5 under applied electric field strength of 800 V/mm.

© 2016 Elsevier Ltd. All rights reserved.

1. Introduction

Polymer actuator technology is being developed for large deformations by repetitive molecular motions. Polymer actuator fall into two groups (Mirfakhrai, Madden, & Baughman, 2007). The first group consists of electronic electroactive polymers (EEPs) in which the dimensional changes occur through electron shifting, an example is the piezoelectric polymer (Mirfakhrai et al., 2007). The second group consists of ionic electroactive polymers (IEAs) (Mirfakhrai et al., 2007) in which the movement of ions is required to make an actuation possible, examples are conductive polymers and polymer gels (Dias et al., 2015). A conductive polymer is one attractive choice to be used to enhance specific electrical and mechanical responses of polymer gels which function as the matrix phase as soft and flexible actuator applications.

Sodium alginates (SA) are anionic biopolymers extracted from brown seaweeds. They are unbranched polysaccharide (Kuen & Mooneya, 2012). Alginates have been extensively investigated and used for many biomedical applications, due to its biocompatibility, low toxicity, relatively low cost, and they can be prepared

through gelation method at room temperature (Kuen & Mooneya, 2012). Polymer hydrogels are three dimensionally crosslinked networks composed of hydrophilic polymers with high water content. Covalent or ionic crosslinking of hydrophilic polymers are typical approaches to form polymer hydrogels, and their properties are highly dependent on the crosslinking type and crosslinking density, in addition to the molecular weight and chemical composition of the polymers (Paradee, Sirivat, Niamlang, & Prissanaroon-Ouajai, 2012). In spite of many advantages, polymer hydrogels still possess many shortcomings, for instance, poor mechanical strength, low strain, low thermal stability, which have restricted their optimal and efficient realization in actuator applications. However, some of these shortcomings can be neutralized by blending with a conductive polymer (Tungkavet, Seetapan, Pattavarakorn, & Sirivat, 2012).

There are several a conductive polymer/biopolymer gel blends that have been developed as actuating materials. Examples are polycarbazole/silk fibroin hydrogel (Srisawasdi, Petcharoen, & Sirivat, 2015), polydiphenylamine/cellulosic gel (Kunchornsup & Sirivat, 2014), poly(3,4 ethylenedioxythiophene)/alginate (Paradee & Sirivat, 2014), and polypyrrole/gelatin hydrogels (Tungkavet et al., 2012).

Polycarbazole (PCB) is one of conductive polymers that contain two six-membered benzene ring fused on sides of a five-membered nitrogen containing ring. It can be synthesized through either

electrochemical or chemical method (Gupta, Singh, & Prakash, 2010). Its applications are for light-emitting diodes, electrochromic displays, organic transistors, and rechargeable batteries (Harun, Saion, Kassim, Yahya, & Mahmud, 2007; Raj, Madheswari, & Ali, 2010; Gupta et al., 2010) due to its high electrical conductivity.

In this work, an electroactive material was fabricated from an SA hydrogel as the matrix phase and embedded with PCB particles. The effects of type and amount of crosslinking, PCB amount, and electric field strength were systematically investigated on the storage modulus response and bending.

2. Material and methods

2.1. Materials

Carbazole (CB) (Synthesis grade, Merck) was used as the monomer. Ammonium persulfate (APS) (AR grade, Sigma-Aldrich) was used as the oxidizing agent. Hydrochloric acid (HCl) 37% and dichloromethane (DCM) (AR grad, Labscan) were used as solvents. Cetyltrimethyl bromide (CTAB) (AR grade, Sigma-Aldrich) was use as surfactants. Ammonium hydroxide (NH$_4$OH) 30% (AR grade, Panreac). Sodium alginates of different molecular weights were used as matrices. Citric acid (AR grade, Merck) was used a covalent crosslinking agent and calcium chloride (AR grad, Fluka,) as an ionic crosslinking agent; both were obtained and used without further purification. Deionized water was used in all experiments.

2.2. Preparation of PCB

PCB was synthesized with CTAB added via interfacial polymerization method (Gupta et al., 2010) using CB monomer, APS, HCl, and DCM. The reaction was carried out at 25 °C. The APS (1.2 M) was dissolved in 50 ml of 0.5 M HCl solution as an aqueous phase. The CB monomer (60 mM) was dissolved in 50 ml of DCM with various monomer: CTAB mole ratios, to finally obtain a non-aqueous phase. Then, the aqueous and non-aqueous solutions were mixed for 24 h to induce CB monomers at the interface between the two immiscible phases. After filtering, the green precipitate was collected and dried in oven at 80 °C for 24 h. Dedoping PCB was performed by stirring the obtained PCB in NH$_4$OH solution of the PCB: NH$_4$OH mole ratio of 1:10 at 25 °C for 24 h. Then, PCB was doped by HClO$_4$ at the HClO$_4$: N$_{PCB}$ mole ratios of 5:1, 10:1, 50:1, and 100:1.

2.3. Preparation of SA hydrogels and PCB/SA blends

SA solutions were prepared from three SA molecular weights namely low molecular weight SA (LSA) of 2.83×10^5 g/mol, medium molecular weight SA (MSA) of 3.34×10^5 g/mol, and high molecular weight SA (HSA) of 4.57×10^5 g/mol in distilled water (1.0% v/v) at 25 °C under continuous stirring for 40 min (Kulkarni, Soppimath, Aminabhavi, Dave, & Mehta, 2000). The crosslinking of SA was carried out by the ionic and covalent crosslinking methods (Kuen & Mooneya, 2012). In case of the ionic crosslinking method, it was prepared by adding the appropriate volume of CaCl$_2$ solution to the SA solution at 25 °C under continuous stirring for 30 min with CaCl$_2$ concentrations varying from 0.0050, 0.0100, 0.0150, and 0.0200% v/v. In case of the covalent method, it was prepared by adding the appropriate volume of citric acid solution to the SA solution at 80 °C under continuous stirring for 30 min with citric acid concentration varying from 0.25, 0.50, 0.75, and 1.0% v/v. The SA mixture solutions were poured into plastic petri dishes (10 cm of diameter). The SA hydrogels were obtained after allowing water evaporation at 25 °C for a period of 2 days and kept at 4 °C for controlling water content in the SA hydrogel samples (~1.5 min in thickness).

The PCB/SA hydrogel blends were prepared by mixing PCB with a SA solution. PCB powder was dispersed in 70 ml SA solution filled with 0.05 M of sodium dodecyl sulfate (SDS) as the surfactant (Srisawasdi et al., 2015) and with 0.015% v/v CaCl$_2$ as the ionic crosslinking agent. The PCB concentration was varied from 0.01, 0.05, 0.1, 0.5, 1.0, 3.0, and 5.0% v/v. The solution was then poured into a plastic petri dish for casting at room temperature for 2 days to obtain the hydrogel blend samples (~1.5 min in thickness).

2.4. Characterizations and testing

2.4.1. The electrical conductivity

The electrical conductivity of the synthesized polycarbazole was determined by pressing the PCB powder into disk pellets under the pressure of 7 kg (diameter of 10 mm and 0.2 mm thickness). Electrical conductivity was measured using a custom-built two-point probe meter connected with a voltage supplier, in which voltage was varied and the resultant current measured in the regime where the resultant current is linearly proportional to the applied voltage, or the linear Ohmic regime. The voltage and the current in the Ohmic regime were converted to the electrical conductivity via Eq. (1):

$$\sigma = 1/\rho = 1/(R_s \times t) = I/(K \times V \times t) \tag{1}$$

where σ is the specific conductivity (S cm^{-1}), ρ is the specific resistivity (Ω cm), R_s is the sheet resistance (Ω sq^{-1}), t is the thickness of the sample pellet (cm), V is the applied voltage (V), I is the measured current (A), and K is the geometric correction factor of the two-point probe meter, K as 4.29×10^{-4}. All sample thicknesses were measured by a thickness gauge (Peacock, PDN-20).

2.4.2. Fourier transform infrared spectrometer

A fourier transform infrared spectrometer, FT-IR (Nicolet, Nexus 670) was used to characterize functional groups of PCB powder, SA and PCB/SA films. For the PCB powder used the in KBr-pellet technique, optical grade KBr (Carlo ErBr Reagent) was used as the background material. The PCB powders were intimately mixed with dried KBr at the PCB:KBr weight ratio of 1:20, then they were compressed into pellets under the force of 7000 kg. The technique used the absorption mode with 32 scans and a resolution of ±4 cm^{-1}, covering a wavelength range of 4000–400 cm^{-1}.

2.4.3. X-ray diffractometer

An X-ray diffractometer, XRD (Rigaku/Smartlab) was used to investigate the degree of crystallinity of the hydrogel samples (sample size: 2 cm^2 square disk with ~1.5 mm in thickness). The diffractometer was operated in the Bragg–Brentano geometry and fitted with a graphite monochromator and the diffracted beam using a 5°/min scan rate.

2.4.4. Thermal gravimetric analyzer

A thermal gravimetric analyzer (DuPont, TGA 2950) was used to determine the amount of water content and the decomposition temperatures of PCB powers, SA hydrogels and PCB/SA hydrogel blends. The thermal behavior was investigated by weighting each sample of 5–10 mg and loaded into a platinum pan and then heating it under nitrogen flow with a heating rate of 10 °C/min from 30 to 800 °C.

2.4.5. Scanning Electron Microscope

A Scanning Electron Microscope, SEM (Hitachi, S4800) was used to examine the morphological structure of PCB and the dispersion of PCB in SA hydrogels. Each sample was placed on the holder with an adhesive tape and with a thin layer of platinum using a JEOL JFC-1100E ion sputtering device for 1 min to observation under SEM. The scanning electron images were obtained by using the acceleration voltage of 10 kV with the magnification of 3.0 k.

2.4.6. Atomic force microscope

An atomic force microscope (AFM) (CSPM, 4000) was used to obtain images to examine the topology of the hydrogels of various crosslinking types and PCB concentrations. The topology images of specimens were taken in the non-contact mode with the cantilever (NSC-14-CrAu) tapping at a scan rate of 0.5 Hz. The electrostatic force microscope (EFM) was determined at signal amplitude of 5 V, and a scan size of $2.5 \times 2.5\,\mu m^2$. The charge distribution and the degree of charge generated were obtained from the EFM technique. In the EFM mode, the sample was scanned twice. First, the tip scanned the surface to obtain the topography images in the non-contact AFM mode associated with the van der Waals fore. The second scan was carried out by the system measuring the tip-surface distance due to the electrostatic force between the material and the probe tip. The electric properties such as the surface potential and the surface charge distribution were obtained from the EFM technique.

2.4.7. Crosslinking density

The crosslinking density of hydrogel was analyzed by the swelling method of Gudeman and Peppas (1995). A sample of the hydrogel (1 cm^2 square, ~1.5 mm in thickness was cut and weighed in air and heptane (a non-polar solvent)). The sample was placed in heptane to obtain the weight in heptane. The sample was then placed in water for 5 days to reach equilibrium, and then was weighed in air and heptane again. Finally, the sample was dried at 25 °C in a vacuum for 5 days. Once again, it was weighed in air and heptane. M_c, the average weight between crosslinks, was calculated from Eq. (2):

$$\frac{1}{\overline{M}_c} = \frac{1}{\overline{M}_n} - \frac{\frac{\bar{v}}{\overline{V}_1}\left[\ln\left(1 - v_{2,s}\right) + v_{2,s} + \chi_1 v_{2,s}^2\right]}{v_{2,.r}\left[\left(\frac{v_{2,s}}{v_{2,r}}\right)^{1/3} - \frac{1}{2}\left(\frac{v_{2,s}}{v_{2,r}}\right)\right]} \qquad (2)$$

where $\overline{M}_n$ is the number-average molecular weight of the polymer before cross-linking, $\bar{v}$ is the specific volume of alginate ($\bar{v}$ = 0.60 cm^3/g of alginate), $\overline{V}_1$ is the molar volume of water (18.1 cm^3/mol), $v_{2,r}$ is the volume fraction of the polymer in a relaxed state, $v_{2,s}$ is the volume fraction of the polymer in solvent state, χ_1 is the Flory polymer-solvent interaction parameter of alginate (χ_1 for alginate is 0.473) (Well & Sheardown, 2011).

2.4.8. Electromechanical properties

A melt rheometer (Rheometric Scientific, ARES) was fitted with a parallel plate fixture (diameter of 25 mm). A DC voltage was applied with a DC power supply (Instek, GFG8216A). A digital multimeter (Tektronix, CDM 250) was used to monitor the voltage input. The samples were prepared in the configuration of Polyimide/Hydrogel/Polyimide sandwich to prevent the shortening of the circuit. In these experiments, the oscillatory shear mode was applied and the dynamic moduli (G′ and G″) were measured as functions of frequency and electric field strength. For each sample, a strain sweep test was first carried out to determine the suitable strains to measure G′ and G″ in the linear viscoelastic regime. The frequency sweep test was then carried out to measure G′ and G″ of each sample as functions of frequency. The frequency was varied from 0.1 to 100 rad/s. Prior to each measurement, the SA and PCB/SA hydrogel blend samples (sample size: 25 mm in diameter, and ~1.5 mm in thickness) were pre-sheared at a low frequency under an electric field for 15 min to ensure equilibrium polarization before the G′ and G″ measurements. Experiments were carried out at the temperature of 300 K and repeated at least three times. The temporal response was investigated with an applied electric field switched on and off periodically at every 600 s, at 800 V/mm. The temporal characteristics were measured in the linear-viscoelastic

regime at a strain of 0.1% and at a frequency of 100 rad/s. For the electromechanical properties of the PCB/SA hydrogel blend, they were carried out with the same procedure as the pristine SA hydrogels.

2.4.9. Dielectrophoresis forces

The dielectrophoresis forces of the SA hydrogels and PCB/SA hydrogel blends (sample sizes: 16.5 mm in length, 3 mm in width, and 1.25 mm in thickness) were determined by measuring the horizontal deflection distances of the specimensin a vertical cantilever fixture. The specimens were vertically suspended and immersed in the silicone oil (viscosity = 100 cSt, conductivity ~10^{-10} S/cm) between parallel copper electrode plates (68 mm of length, 40 mm of width, and 2 mm of thickness). The gap between the electrode pair was fixed at 38 mm. A DC voltage was applied with a DC power supply (Goldsun, GPS 3003B) connected to a high voltage power supply (Gamma High Voltage, UC5-30P and UC5-30N). A video camera was used to record the movement during experiment. Pictures were captured from a video camera and the deflection distances in x (d) and y axes (l) at the end of the specimen were determined by using the Scion Image software (version 4.0.3). The electric field strength was varied between 0 and 500 V/mm at the room temperature of 300 K. Both the voltage and the current were monitored. The resisting elastic force of the specimens were calculated under electric field using the non-linear deflection theory of a cantilever (Sato, Watanabe, & Osaki, 1996) which was obtained from the standard curve between $(F_e l_0^2)/(EI)$ and d/l_0 (l_0 = initial length of specimens); F_e is the elastic force, d is the deflection distance in the horizontal axis, l is the deflection distance in the vertical axis, E is the Young's modulus which is equal to $2G'(1 + \nu\nu)$, where G′ is the shear storage modulus taken to be G′ ($\omega = 1$ rad/s) at various electric field strengths, is the Poisson's ratio (0.5 for an incompressible sample), and I is the moment of inertia $(1/12)t^3 w$, where t is the thickness of the sample, and w is the width of the sample. The electrophoresis force was calculated from the static horizontal force balance consisting of the elastic force, the corrective gravity force (mg tan θ), and the buoyancy force (ρV g tan θ) as shown in Eq. (3):

$$F_d \approx F_e + mg\left(\tan\theta\right) - \rho Vg\left(\tan\theta\right) \qquad (3)$$

where g is 9.8 m/s^2, m is the mass of the specimen, and θ is the deflection angle, ρ is the density of the fluid (silicon oil = 0.97 g/cm^3), and V is the volume of the displaced fluid.

3. Results and discussion

3.1. Characterization of PCB

The FT-IR spectrum of the PCB was taken to identify the characteristic absorbance peaks. The characteristic peaks appeared at 3400 cm^{-1}, 1600–1625 cm^{-1}, 1400–1489 cm^{-1}, 1200–1235 cm^{-1}, 800–875 cm^{-1}, and 700–750 cm^{-1}. These peaks can be assigned to the N—H stretching of hetero-aromatics, the C—H in plane bending, the C—H deformation of tri-substituted benzene ring, and the C—H out-of-plane bending, respectively (see Fig. S1 in the Supplementary materials) (Gupta et al., 2010; Raj et al., 2010; Zhuo, Du, Li, Sun, & Ying Chu, 2013).

The morphology of PCB synthesized via interfacial polymerization was investigated with and without surfactant (CTAB). For the PCB synthesized without CTAB, the particle shape of PCB is a hollow spheres structure (Fig. 1A) due to vesicle micelle forming from CB monomers (Gupta et al., 2010). For the PCB synthesized with CTAB, the particle shape is a connected hollow spheres structure at the CTAB concentration more than $2 \times$ CMC (monomer: CTAB mole ratio of 1:0.00136) (Fig. 1B) due to the reverse micelle formation of a CTAB (Holmberg, Jonsson, Kronberg, & Lindman, 2003;
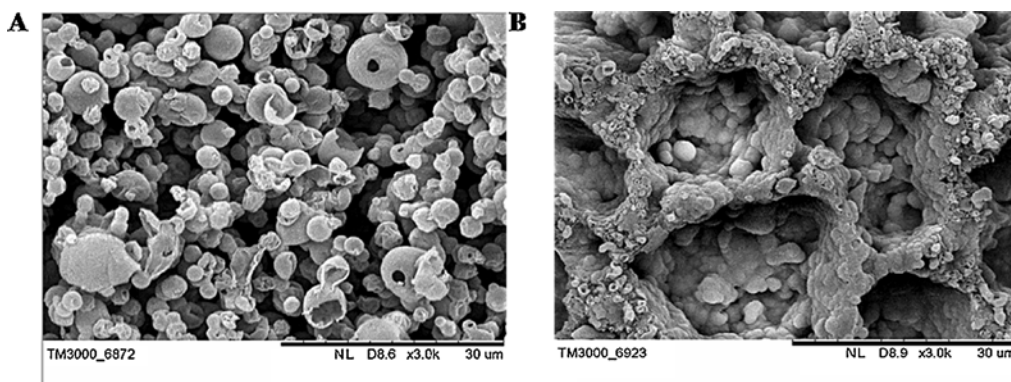
Fig. 1. SEM photographs of PCB synthesized by interfacial polymerization: (A) PCB without CTAB; and (B) PCB: CTAB mole ratio of 1:0.0136 (more than $2 \times$ CMC) at 24 h.

Zingaretti et al., 2003; Pattavarakorn et al., 2013; Zhang et al., 2014). The formation of the spherical PCB occurs outside the reverse micelles. So, the reverse micelles generate pore spaces within the system and produce a fusion and aggregation of the hollow spheres. The mechanism is however the same as the system without CTAB (Gupta et al., 2010). The particle sizes of a hollow sphere structure and a connected hollow spheres structure were 3213 ± 944 and 2068 ± 455 nm, respectively.

The electrical conductivity values of the doped hollow sphere structure and the doped connected hollow spheres structure were $(5.59 \pm 0.27) \times 10^{-2}$ and 11.3 ± 0.36 S/cm, respectively. The electrical conductivity was thus increased by three orders of magnitude relative to the doped hollow spheres structure. Therefore, a connected hollow spheres structure of PCB (synthesized with CTAB) was chosen to further prepare PCB/SA hydrogel blends.

3.2. Crosslinking density of SA hydrogel

The crosslinked SA hydrogels were prepared by two different crosslinking methods namely the ionic crosslinking from calcium chloride ($CaCl_2$) and the covalent crosslinking from citric acid (CA). In the case of SA hydrogels crosslinked with $CaCl_2$, the crosslinking density increased by a factor of two with increasing $CaCl_2$ concentration from 0.005 to 0.02% v/v. For the effect of SA molecular weight, a lower molecular weight SA possessed a higher crosslinking density compared with the others because a shorter molecular chain has a larger free volume and chain ends that facilitate an easy attachment between the Ca^{2+} ions and the functional groups of SA (Stone, Gosavi, Athauda, & Ozer, 2013). Similarly, the crosslinking density of SA hydrogels crosslinked with CA increased with CA concentration by about 8 times with SA concentration varying from 0.25 to 1.00% v/v.

On comparing the two crosslinking methods, the CA system provided a higher crosslinking density than the $CaCl_2$ system because the carboxyl group of CA molecule can permanently reacted with the carboxyl group of SA molecule as a covalent bonding (Stone et al., 2013). While Ca^{2+} ions form a physical bond with SA molecule (Paradee & Sirivat, 2014). When crosslinked SA hydrogels were swollen in the water for evaluating the crosslinking density, the physical bond was easily destroyed and water easily penetrated through the specimens causing a large amount of weight loss (Kuen & Mooneya, 2012).

The crosslinking densities of the SA hydrogels from the two crosslinking methods were nearly the same at 0.015% v/v of $CaCl_2$ and 0.50% v/v of CA. The values were 15×10^{-6} to 20×10^{-6} mol/cm^3, respectively. Thus, these two samples were used in further studies.

3.3. Fourier transform infrared spectroscopy

The characteristic FT-IR spectrum of HSA hydrogels, indicate the peak of the —OH stretching at 3265 cm^{-1}, the —COO^- stretching at 1590–1587 cm^{-1}, the C—C and C—O stretching at 1771 cm^{-1}, the C—C stretching at 1025 cm^{-1}, and the C—H stretching at 800–815 cm^{-1} (Saarai, Kasparkova, Sedlacek, & Saha, 2013). As can be see, the positions of the —COO^- and —OH bands shift and the vibration intensities apparently decrease with the addition of $CaCl_2$, implying that both the —COO^- and —OH groups on SA molecules are preferentially coordinated with calcium ions (Ca_2^+) in the $CaCl_2$ solution (Wang, Liu, Li, & Pan, 2009). Moreover, the positions of the —COO^- and —OH bands shift and the vibration intensities apparently decrease with the addition of CA, implying that both the —COO^- and —OH groups on SA molecules are covalently crosslinked with the —COO^- and —OH groups of CA (see Fig. S2 in the Supplementary materials).

3.4. X-ray diffractometer

The amount of crystallinity of SA hydrogels was characterized by the XRD technique. The results show the diffraction peaks before and after the crosslinking process of SA hydrogels (see Fig. S3 in the Supplementary materials). It can be observed that the crystallinity of SA hydrogel decreases after crosslinking by $CaCl_2$ and CA as the crosslinking obstructed the SA chain packing Li, Fang, Vreeker, & Appelqvist, 2007).

Moreover, the crystallinity of SA hydrogels with the covalent crosslinking is higher than the ionic crosslinking method, as evidenced by a shaper peak and a higher intensity of the diffraction peak around 30°. This is because the chemical crosslinking agent provides a greater molecular chains packing efficiency when compared with the physical bonding (Gupta et al., 2010). The order orientation of SA molecules as obtained from the crosslinking with citric acid is also higher leading to a greater chain alignment and crystallinity.

3.5. Thermal gravimetric analysis

The thermograms show the water contents of the SA hydrogels with the ionic crosslinking and covalent crosslinking methods. The data indicate an initial weight loss of approximately 90 wt% as temperature increases to 100 °C, corresponding to the loss of water (see Fig. S4 in the Supplementary materials). In addition, the degradation of SA molecule occurs in the degradation temperature ($T_{d,onset}$) range of 200–230 °C depending on SA molecular weight.

Moreover, the weight loss of HSA hydrogels decreases with increasing PCB content because of the Van der Waals force and the hydrogen bonding interaction between HSA and PCB
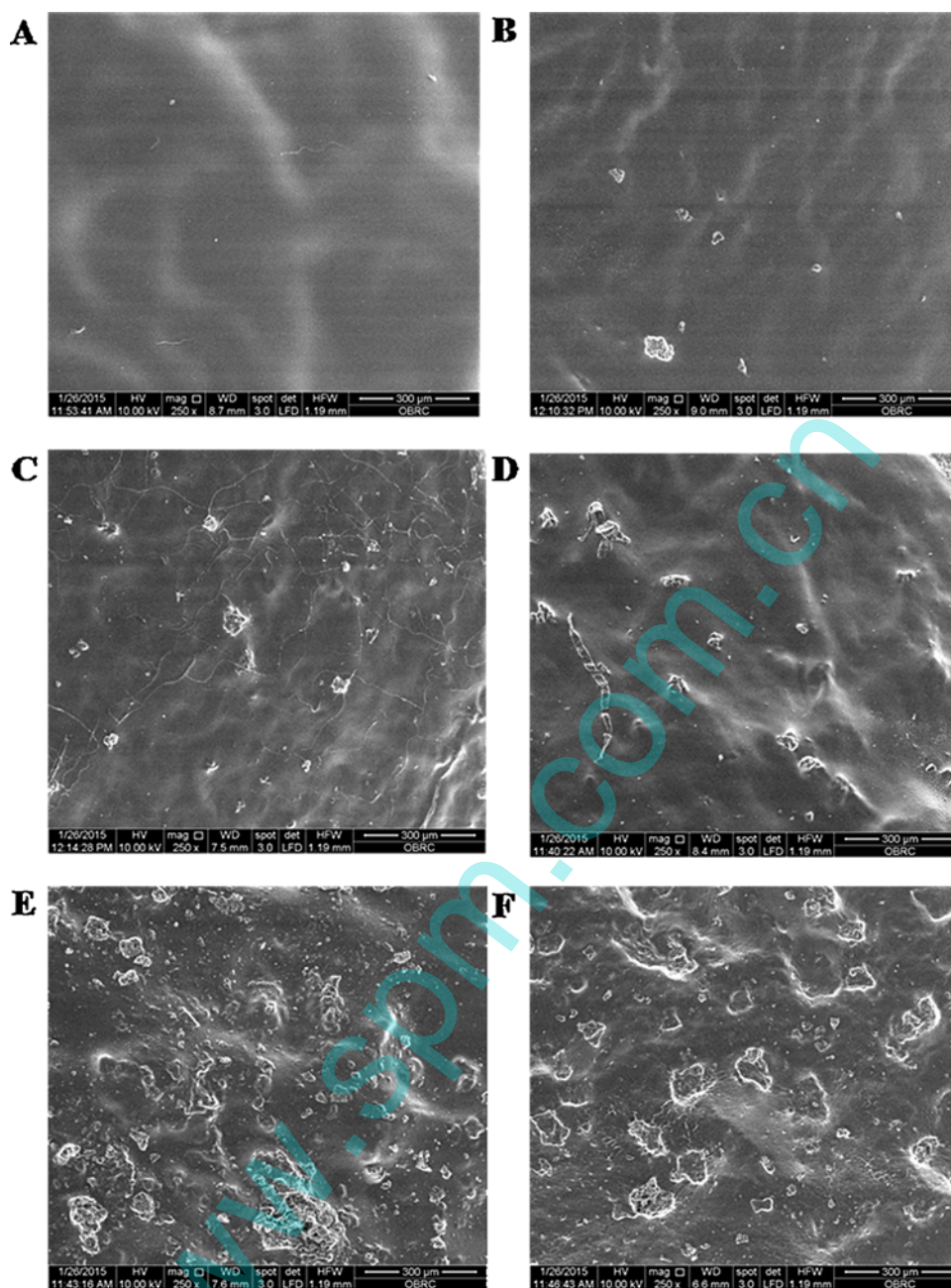
Fig. 2. SEM photographs of PCB/HSA hydrogel blends of various PCB concentrations: (A) pristine HSA; (B) 0.01% v/v PCB; (C) 0.05% v/v PCB; (D) 0.10% v/v PCB; (E) 0.30% v/v PCB; and (F) 0.50% v/v PCB.

(Petcharone & Sirivat, 2013). $T_{d,onset}$ of the PCB/HSA blends increases with increasing PCB because of higher $T_{d,onset}$ of PCB (Gupta et al., 2010).

3.6. Scanning Electron Microscope

Fig. 2 shows SEM micrographs of the PCB/HSA hydrogel blends of various PCB concentrations. The micrographs show a moderate PCB dispersion in the HSA hydrogel at low PCB concentration; the dispersion becomes poorer at a high PCB concentration (concentration of PCB beyond 0.1% v/v). A moderately well dispersed PCB/HSA hydrogel blend was obtained because of the Van der Waals force and the hydrogen bonding interaction between PCB and HSA hydrogel (Tungkavet et al., 2012).

3.7. Atomic force microscope

The topology of SA hydrogels of various crosslinking types was investigated by topology in EFM technique as shown in Fig. 3. Fig. 3A shows a smooth phase with some small bright areas that can be referred to a low electrostatic force under applied electric field. The bright regions can be assigned to the presences of negative charges namely COO^- on the HSA surface which provides the attractive force between the positively charged EFM tip and the negatively charged HSA surface.

For the HSA hydrogels with crosslinking, a higher force response to electric field is obtained, where the bright regions are more abundant as shown in Fig. 3B and C. Between the ionic and covalent crosslinkings, the ionic crosslinking of $CaCl_2$ shows continuously brighter areas (Fig. 3B) of eggs shell block like due to the forma-
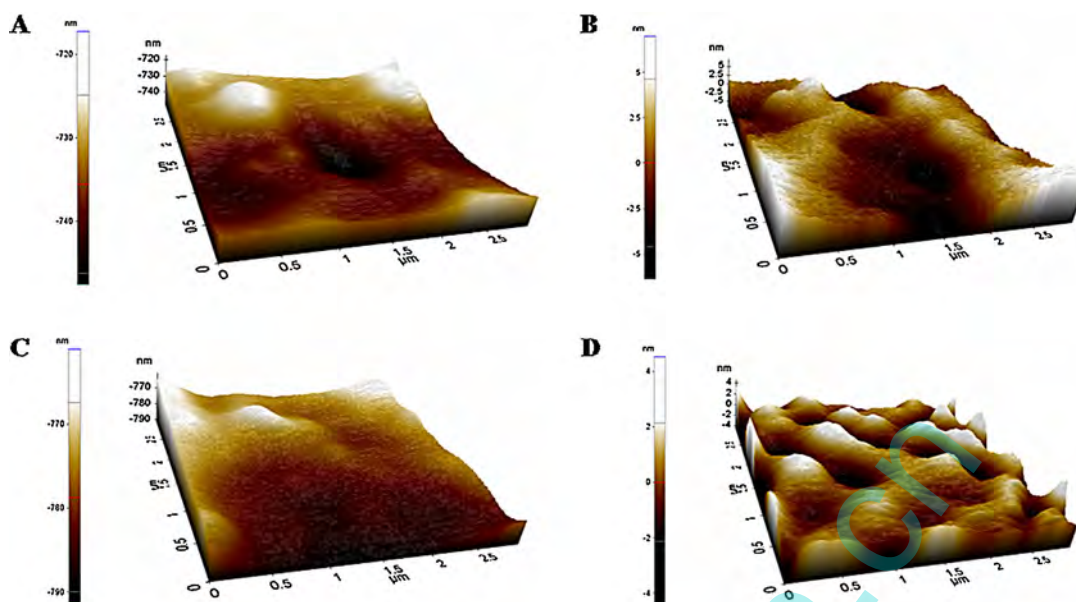
Fig. 3. EFM images ($2.5 \times 2.5\ \mu m^2$): (A) HSA without crosslinking; (B) 1% v/v HSA + 0.015% v/v CaCl$_2$; (C) 1% v/v HSA + 0.50% v/v CA; and (D) 0.01% v/v PCB/HSA + 0.015% v/v CaCl$_2$ hydrogel blend.

tion of Ca^{2+} in HSA hydrogel (Kuen & Mooneya, 2012). In the case of covalent crosslinking, the existence of COO$^−$ from CA is shown as bright regions as well (Petcharone & Sirivat, 2013; Saarai et al., 2013).

When HSA is added with PCB, the anionic phase becomes a more brilliant phase as PCB is acting as a conductive polymer with more free electrons present (Fig. 3D) (Tungkavet et al., 2012).

3.8. Time dependence of the electromechanical response

The temporal characteristics of a HSA hydrogel by ionic crosslinking, a HSA hydrogel by covalent crosslinking and a PCB/HSA hydrogel by ionic crosslinking at PCB concentration of 0.1% v/v at electric field strength of 800 V/mm were investigated in which the electric field was turn on and off (alternately at every 600 s) periodically during the total experiment period of 8000 s. The temporal characteristic of each sample was recorded in the linear viscoelastic regime at a strain of 0.1%, frequency of 100 rad/s, and at temperature of 300 K.

Fig. 4A shows a comparison of the storage modulus (G′) during the time sweep test. For all samples, G′ increases rapidly when the electric field is on due to the polarization of HSA molecules (Tungkavet et al., 2012), and decreases instantaneously when the electric field is off. The G′ attains the steady states at different actuating cycles; the HSA hydrogel by ionic crosslinking takes 3 cycles, the HSA hydrogel by covalent crosslinking requires 2 cycles, but PCB/HSA only takes 1 cycle to reach their steady states. The HSA hydrogel by the ionic crosslinking requires the longest response time to reach the steady state because the ionic crosslinking is a physical interaction. The carboxylic groups and ions are allowed to move or rotate within the specimen leading to a longest time for the equilibrium polarization under electric field and neutral polarization without electric field. The HSA hydrogel by the covalent crosslinking requires a shorter time to reach the steady state than the HSA hydrogel by the ionic crosslinking because the covalent crosslinking is a chemical interaction between the carboxylic group of SA and the carboxyl group of citric acid (Kunchornsup & Sirivat, 2010; Tungkavet et al., 2012). The polar groups of SA are restricted in movement leading to a shorter time for the equilibrium polarization under electric field and neutral polarization without electric
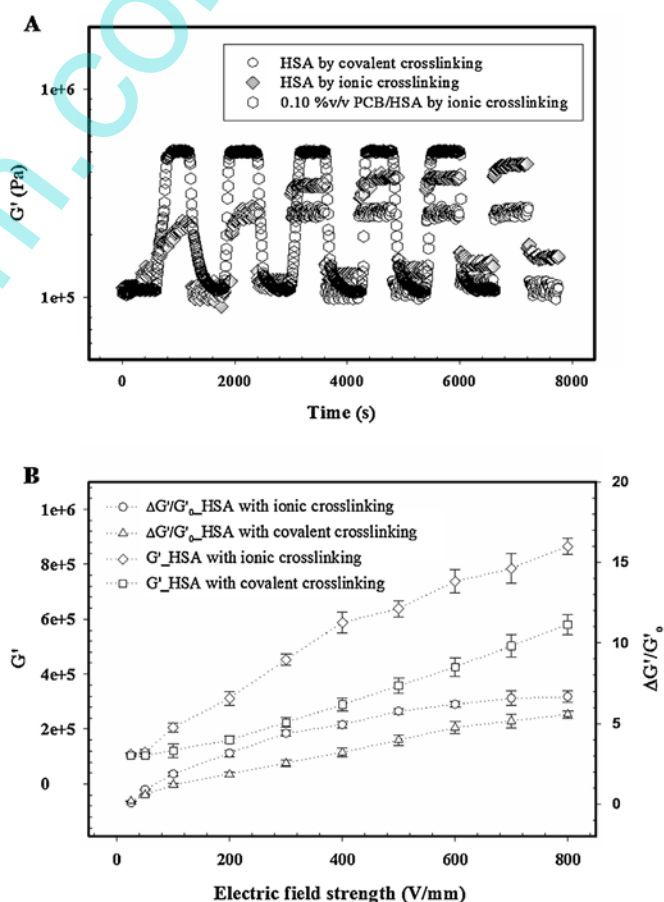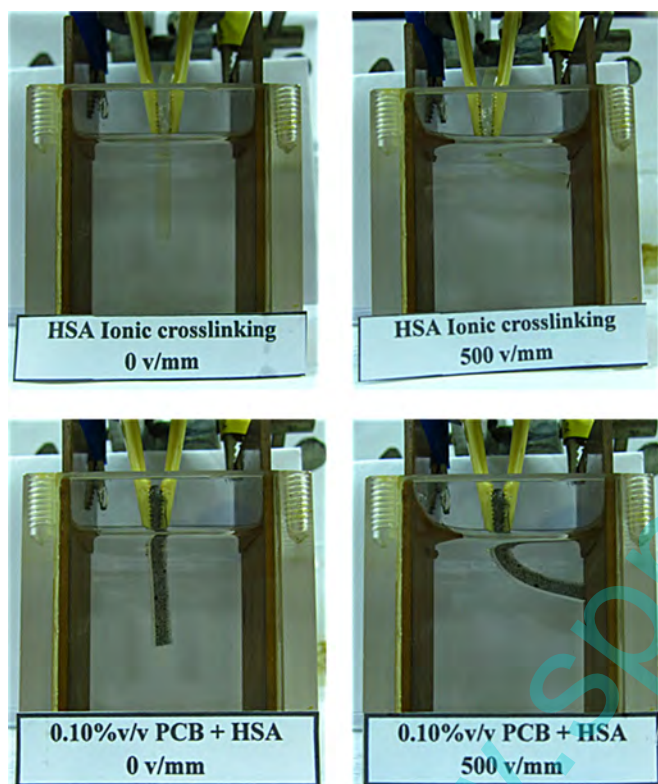

Fig. 4. The electromechanical properties of 1% v/v HSA with ionic and covalent crosslinking at strain of 0.1%, frequency of 100 rad/s and at 300 K: (A) temporal at an electric field strength of 800 V/mm; and (B) the storage modulus (G′) and storage modulus sensitivity ($\Delta G'/G'_0$) versus an electric field strength.

field (Tungkavet et al., 2012). After adding PCB in HSA hydrogel, the PCB/HSA hydrogel blend requires a shortest response time to reach

Table 1
Comparison of electromechanical properties of the SA hydrogels and PCB/HSA hydrogel blends at frequency of 100 rad/s, an electric field strength of 800 V/mm, and at 300 K.

Samples	Initial storage modulus (G'_o, Pa)	Storage modulus (G', Pa)	Storage modulus sensitivity ($\Delta G'/G_o$)
1% v/v HSA + 0.015% v/v CaCl$_2$	$1.09 \times 10^5 \pm 1.49 \times 10^4$	$8.16 \times 10^5 \pm 3.81 \times 10^4$	7.66 ± 0.35
1% v/v MSA + 0.015% v/v CaCl$_2$	$8.58E + 10^4 \pm 3.07 \times 10^3$	$5.35 \times 10^5 \pm 2.41 \times 10^4$	6.20 ± 0.28
1% v/v LSA + 0.015% v/v CaCl$_2$	$2.51 \times 10^4 \pm 9.38 \times 10^3$	$2.51 \times 10^5 \pm 9.38 \times 10^3$	3.37 ± 0.33
1% v/v HSA + 0.50% v/v CA	$1.10 \times 10^5 \pm 6.69 \times 10^3$	$6.89 \times 10^5 \pm 5.51 \times 10^4$	5.36 ± 0.43
1% v/v MSA + 0.50% v/v CA	$9.50E + 10^4 \pm 7.60 \times 10^3$	$6.10 \times 10^5 \pm 4.88 \times 10^4$	5.02 ± 0.40
1% v/v LSA + 0.50% v/v CA	$9.76 \times 10^4 \pm 7.81 \times 10^3$	$3.06 \times 10^5 \pm 9.38 \times 10^3$	2.12 ± 0.17
0.01% v/v PCB/HSA + 0.015% v/v CaCl$_2$	$3.22 \times 10^4 \pm 2.57 \times 10^3$	$4.44 \times 10^5 \pm 3.55 \times 10^4$	12.80 ± 1.02
0.05% v/v PCB/HSA + 0.015% v/v CaCl$_2$	$3.25 \times 10^4 \pm 2.60 \times 10^3$	$5.27 \times 10^5 \pm 4.22 \times 10^4$	15.21 ± 1.22
0.10% v/v PCB/HSA + 0.015% v/v CaCl$_2$	$3.30 \times 10^4 \pm 2.64 \times 10^3$	$6.26 \times 10^5 \pm 5.01 \times 10^4$	18.55 ± 1.48
0.30% v/v PCB/HSA + 0.015% v/v CaCl$_2$	$3.32 \times 10^4 \pm 2.66 \times 10^3$	$4.21 \times 10^5 \pm 3.37 \times 10^4$	12.15 ± 0.97
0.50% v/v PCB/HSA + 0.015% v/v CaCl$_2$	$5.02 \times 10^4 \pm 4.01 \times 10^3$	$1.44 \times 10^5 \pm 1.15 \times 10^4$	4.33 ± 0.35

Fig. 5. Bending of pristine HSA hydrogel and 0.10% v/v PCB/HSA hydrogel blend at electric field strength 0 and 500 v/mm.

the steady state because the PCB generates a particle-matrix interaction and the reduced the free volume inside the specimen leading to a shortest time for the equilibrium polarization under electric field and neutral polarization without electric field (Petcharoen & Sirivat, 2016).

3.9. Electromechanical properties

The electromechanical properties of SA hydrogels were characterized by the melt rheometer under oscillatory shear mode at 300 K. The strain sweep tests were first carried out to determine an appropate strain for measuring the G' in a linear viscoelastic regime. The appropriate strain value used in the linear viscoelastic regime of 1% v/v HSA, 1% v/v MSA, and 1% v/v LSA hydrogel crosslinked with 0.015% v/v CaCl$_2$ and 0.50% v/v CA was 0.1%.

Fig. 4B shows the G' and $\Delta G'/G'_0$ vs. electric field of 1% v/v HSA hydrogels crosslinked by 0.015% v/v CaCl$_2$ and crosslinked by 0.50% v/v CA, respectively, at frequency 100 rad/s, an electric field strength of 800 V/mm, and at 300 K. The dataclearly show that

when the electric field is applied, the G' increases because of the polalization of carboxylic groups on the SA chainsand ions inside the hydrogel (Dias et al., 2015; Hiamtup, Sirivat, & Jamieson, 2008; Niamlang & Sirivat 2008; Gupta et al., 2010; Kunchornsup & Sirivat, 2014). This in turn reduces the chain free movements and enhance the chain rigidity. Moreover, the G' and $\Delta G'/G'_0$ of the samples increase with increasing the molecular weight of SA as shown in Table 1. As the molecular weight of SA increases, the number density of carboxylic groups increases leading to a higher polarization nunder applied electric field (Kunanuruksapong & Sirivat, 2008; Niamlang & Sirivat, 2008; Thipdech, Kunanuruksapong, & Sirivat, 2008; Tungkavet et al., 2012). However, the loss modulus (G'') also increased with increasing electric field strength and SA molecular weight due to the polarization of water ions and hydrogen bonding between SA and water (Thongsak, Kunanuruksapong, Sirivat, & Lerdwijitjarud, 2011).

At the electric field of 800 V/mm, the highest molecular weight SA showed the highest $\Delta G'/G'_0$ values namely 7.66 and 6.20 for the ionic crosslink and covalent crosslink, respectively. For the lowest molecular weight, the $\Delta G'/G'_0$ values for the ionic crosslink and covalent crosslink were 3.37 and 2.12, respectively. From this result, it can be concluded that a higher molecular weight containing a larger amount of polar groups provides a better electromechanical response compared to those of the low molecular weight.

For the $\Delta G'/G'_0$ of SA from ionic crosslinking and covalent crosslinking, the $\Delta G'/G'_0$ of the ionic crosslinking is higher than the covalent crosslinking because the ionic crosslinking is a physical interaction. The carboxylic groups and ions are allowed to move or rotate within the specimen. The covalent crosslinking is a chemical interaction between the carboxylic group of SA and the carboxyl group of citric acid (Kunchornsup & Sirivat, 2010; Tungkavet et al., 2012). The polar groups of SA are restricted in movement leading to a lower electromechanical response (Tungkavet et al., 2012).

In comparison with other electroactive polymers, the uncrosslinked high-gel-strength gelatin exhibited the storage modulus sensitivity of 2.30 (Tungkavet et al., 2012). Both types of the crosslinked SA hydrogels possess the superior responses and sensitivity values which are an order of magnitude greater than those of the triblock polymers and gelatins.

The $\Delta G'/G'_0$ vs. electric field of PCB/HSA hydrogel blends by ionic crosslinking (0.015% v/v CaCl$_2$) of various PCB concentrations of 0.01% v/v, 0.05% v/v, 0.10% v/v, 0.03% v/v, and 0.50% v/v, respectively, at frequency of 100 rad/s, electric field strength of 800 V/mm and at 300 K. The data show that when the PCB is introduced into the system at 0.01% v/v, 0.05% v/v, and 0.10 % v/v, the G' increases at a given electric field strength. The highest $\Delta G'/G'_0$ obtained is amazingly high as 18.55 for the 0.10% v/v PCB/HSA hydrogel blend. This is because the PCB acts as a conductive polymer which produces additional electrons polarization and dipole interaction as well as enhances the polarization within the PCB/HSA
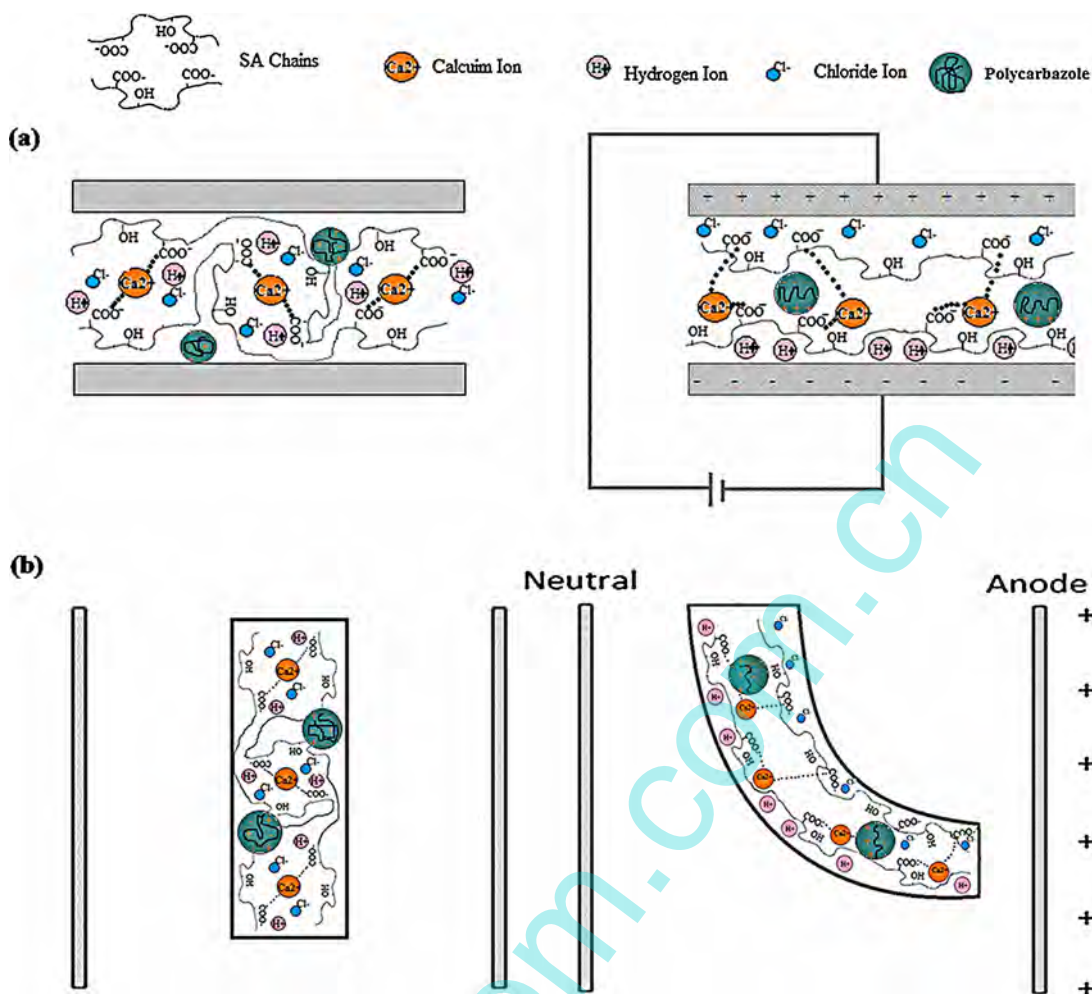
Fig. 6. Schematics of polarized carboxyl groups, ions, and PCB in PCB/HSA hydrogel blends with applied an electric field: (A) electrostriction, and (B) dieletrophoresis.

Table 2
Deflection angles, deflection distances, and dielectrophoresis forces of SA hydrogels and PCB/HSA hydrogel blend at an electric field strength of 500 V/mm.

Samples	Electric field strength (V/mm)	Deflection angle (degree)	Deflection distance (mm)	Dielectrophoresis force (mN)
1% v/v HSA + 0.015% v/v CaCl$_2$		55.58 ± 0.23	17.10 ± 0.57	1.00 ± 0.01
1% v/v HSA + 0.50% v/v CA		46.15 ± 0.39	15.31 ± 0.42	0.75 ± 0.02
0.01% v/v PCB/HSA + 0.015% v/v CaCl$_2$		40.11 ± 1.76	14.00 ± 0.99	1.78 ± 0.17
0.05% v/v PCB/HSA + 0.015% v/v CaCl$_2$	500	40.34 ± 1.64	14.35 ± 0.35	1.83 ± 0.01
0.10% v/v PCB/HSA + 0.015% v/v CaCl$_2$		44.19 ± 0.13	15.75 ± 0.07	2.76 ± 0.15
0.30% v/v PCB/HSA + 0.015% v/v CaCl$_2$		36.69 ± 2.85	12.60 ± 0.99	2.18 ± 0.02
0.50% v/v PCB/HSA + 0.015% v/v CaCl$_2$		24.29 ± 0.17	8.89 ± 0.07	1.06 ± 1.16

hydrogel blends (Ludeelerd, Niamlang, Kunaruksapong, & Sirivat, 2010; Tangboriboon et al., 2010; Tangboriboon, Longtong, Sirivat, & Kunanuraksapong, 2011; Tungkavet et al., 2012; Tangboriboon, Mulsow, Kunchornsup, & Sirivat, 2013). The Schematics of polarized carboxyl groups, ions, and PCB in PCB/HSA hydrogel blends with applied an electric field of an electrostriction are shown in Fig. 6A. At a PCB concentration higher than 0.10% v/v, the PCB generates the PCB aggregation leading to the partial phase separation between the PCB and HSA where it reduces the interaction between PCB particles and the SA matrix. The poor particle-matrix interaction produces a week interfacial intermolecular interaction (Petcharoen & Sirivat, 2016; Puvanatvattana et al., 2006; Tangboriboon et al., 2011; Tungkavet et al., 2012).

Tungkavet et al. (2012) reported a similar effect for a nanowire Ppy/gelatin system. The maximum $\Delta G'/G'_0$ occured with the 0.1 vol% nanowire Ppy/gelatin hydrogel. However, the $\Delta G'/G'_0$

decreased with the nanowire Ppy/gelatin concentration 1.0 vol% because of the phase separation between the gelatin hydrogel and the nanowire Ppy agglomeration. Liu and Shaw (2001) reported the effect for a silica/silicone system. The enhancement of shear modulus was negligible below 8.0 vol%, but increased dramatically above this threshold concentration. At a volume amount above 55.0 vol%, the shear modulus decreased since the interparticle force decreased with the steric hindrance effect (Liu & Shaw, 2001).

The response speeds are important characteristics of an electroactive material with can be identified as the induction time (τ_{ind}) and recovery time (τ_{rec}), the times required for G' to reach and decay toward its on and off steady states, respectively. The HSA hydrogel by ionic crosslinking, the HSA hydrogel by covalent crosslinking and the PCB/HSA hydrogel blend possess the induction times, the time at which the storage modulus increase and attains a steady state value, of 248, 210 and 374 s, respectively and the recov-

ery times, the time at which the storage modulus decreases and reaches a steady state value, of 222, 200 and 283 s, respectively. The HSA hydrogel by ionic crosslinking has the higher induction time (τ_{ind}) and recovery time (τ_{rec}) than the HSA hydrogel crosslinked by covalent crosslinking because the ionic crosslinking is a physical interaction. The carboxylic groups and ions are allowed to move or rotate within the specimen leading to the longer time for the equilibrium polarization under electric field and neutral polarization without electric field. But, the covalent crosslinking is a chemical interaction between the carboxylic group of SA and the carboxyl group of citric acid. The polar groups of SA are restricted in movement leading to shorter time for the equilibrium polarization under electric field and neutral polarization without electric field. The PCB/HSA hydrogel blend has the longest induction time (τ_{ind}) and recovery time (τ_{rec}), because the PCB acts as a conductive polymer which produces additional electronic and molecular polarizations leading to the longest time for the equilibrium polarization under electric field and neutral polarization without electric field.

3.10. Deflection responses

The deflection responses of HSA hydrogel and 0.10% v/v PCB/HSA hydrogel blend with and without an electric field strength of 500 V/mm are shown in Fig. 5. Upon applying an electric field, the free lower ends of the hydrogels deflect toward the positive electrode, with the amounts depending on the electric field strength. The deflection responses suggest the polarized carboxyl groups and ions, in which the HSA structures possess a net negative charge. Another mechanism for the deflection arises from the dieletrophoresis force originated from the polarizable body in a nonuniform electric field (Voldman, 2006). The deflection distances, deflection angles and dielectrophoresis forces of the HSA hydrogel and the PCB/HSA hydrogel blend are shown in Table 2. The HSA hydrogel shows a greater deflection distance value and deflection angle than the PCB/HSA hydrogel blends. The addition of PCB produces an additional rigidity into the blends. However, the PCB/HSA hydrogel blends show a higher dielectrophoresis forces at a given electric field strength relative to the HSA hydrogel. The highest dielectrophoresis force belongs to the 0.1% v/v PCB blend because PCB acts as a conductive polymer with additional electrons polarization and dipole interaction as well as enhances the polarization within the PCB/HSA hydrogel blends (Niamlang & Sirivat, 2008; Tungkavet et al., 2012). The schematics of polarized carboxyl groups, ions, and PCB in PCB/HSA hydrogel blends with applied an electric field of electrostriction is shown in Fig. 6B. At a higher PCB concentration, the dielectrophoresis force decreases because of the partial PCB aggregation reducing polarizability and the intermolecular interaction (Kunanuruksapong & Sirivat, 2011; Tungkavet et al., 2012). Similarly, the deflection distance and deflection angle also decrease because of the higher initial rigidity and the PCB agglomeration (Kunanuruksapong, & Sirivat, 2011). The dielectrophoresis forces at the electric field strength of 500 V/mm of the HSA, 0.01% v/v PCB/HSA, 0.05% v/v PCB/HSA, 0.10% v/v PCB/HSA, 0.50% v/v PCB/HSA, 0.10% v/v PCB/HSA, 0.30% v/v PCB/HSA, and 0.50% v/v PCB/HSA hydrogel blends are 1.00, 1.78, 1.83, 2.76, 2.18 and 1.06 mN, respectively. Moreover, the bending responses are nearly the same after the repeating cycles more than 20 cycles as shown in Figs. S5 and S6 in Supplementary materials.

In comparison with previous work, the maximum dielectrophoresis force at 600 V/mm of a gelatin hydrogel was 7.05 mN (Tungkavet et al., 2012). The dielectrophoresis force of a cellulosic gel at 500 V/mm was 4.63 mN (Kunchornsup & Sirivat, 2012). The present HSA and PCB/HSA systems possess the dielectrophoresis forces of the same order of magnitude as other hydrogels.

4. Conclusions

The electromechanical properties, and the cantilever bending of the SA hydrogels and PCB/HSA hydrogel blends were investigated at electric field strength varying from 0 to 800 V/mm. For the SA hydrogels, the $\Delta G'$ and $\Delta G'/G'_0$ increased dramatically with increasing electric field strength. The $\Delta G'$ and $\Delta G'/G'_0$ of SA hydrogels with ionic crosslinking were higher than those of the SA hydrogels with covalent crosslinking. Moreover, the $\Delta G'$ and $\Delta G'/G'_0$ of the SA hydrogels increased with increasing molecular weight of SA.

For the PCB/HSA hydrogel blend, the $\Delta G'/G'_0$ increased with increasing PCB concentration; it was the highest with the 0.10% v/v PCB/HSA, but it decreased at PCB concentrations higher than 0.10% v/v due to the partial PCB agglomeration.

In the deflection measurement, the deflection distances and the dielectrophoresis forces of the HSA hydrogel and PCB/HSA hydrogel blends increased monotonically with increasing electric field strength. The PCB/HSA hydrogel blends showed higher dielectrophoresis forces due to the additional polarizability but lower deflection distances relative to those of the pristine HSA hydrogels due to the additional rigidity introduced.

Appendix A. Supplementary data

Supplementary data associated with this article can be found, in the online version, at http://dx.doi.org/10.1016/j.carbpol.2016.05.077.

References

Dias, J. C., Lopes, A. C., Magalhaes, B., Botelho, G., Silva, M. M., Esperanca, J. M. S. S., & Lanceros-Mendez, S. (2015). High performance electromechanical actuators based on ionic liquid/poly(vinylidene fluoride). *Polymer Testing, 48*, 199–205.

Gudeman, L. F., & Peppas, N. A. (1995). pH-Sensitive membranes from poly(vinyl alcohol)/poly(acrylic acid) interpenetrating networks. *Journal of Membrane Science, 107*, 239–248.

Gupta, B., Singh, A. K., & Prakash, R. (2010). Electrolyte effects on various properties of polycarbazole. *Thin Solid Films, 519*, 1016–1019.

Harun, M. H., Saion, E., Kassim, A., Yahya, N., & Mahmud, E. (2007). Conjugated conducting polymers: a brief overview. *JASA, 2*, 63–68.

Hiamtup, P., Sirivat, A., & Jamieson, A. M. (2008). Electromechanical response of a soft and flexible actuator based on polyaniline particles embedded in a cross-linked poly(dimethyl siloxane) network. *Materials Science and Engineering C, 28*, 1044–1051.

Holmberg, Jonsson, B., Kronberg, B., & Lindman, B. (2003). *Surfactants and polymers in aqueous solution* (2nd ed.). West sussex: Chichester.

Kuen, Y. L., & Mooneya, D. J. (2012). Alginate: properties and biomedical applications. *Polymer Science, 37*, 106–126.

Kulkarni, A. R., Soppimath, K. S., Aminabhavi, T. M., Dave, A. M., & Mehta, M. H. (2000). Glutaraldehyde crosslinked sodium alginate beads containing liquid pesticide for soil application. *Journal of Controlled Release, 63*, 97–105.

Kunanuruksapong, R., & Sirivat, A. (2008). Electrical properties and electromechanical responses of acrylic elastomers and styrene copolymers: effect of temperature. *Applied Physics A, 92*, 313–320.

Kunanuruksapong, R., & Sirivat, A. (2011). Effect of dielectric constant and electric field strength on dielectrophoresis force of acrylic elastomers and styrene copolymers. *Current Applied Physics, 11*, 393–401.

Kunchornsup, W., & Sirivat, A. (2010). Effects of crosslinking ratio and aging time on properties of physical and chemical cellulose gels via1-butyl-3-methylimidazolium chloride solvent. *Journal of Sol-Gel Science and Technology, 56*, 19–26.

Kunchornsup, W., & Sirivat, A. (2012). Physically cross-linked cellulosic gel via 1-butyl-3-methylimidazolium chloride ionic liquid and its electromechanical responses. *Sensors & Actuators A, 175*, 155–164.

Kunchornsup, W., & Sirivat, A. (2014). Electromechanical properties study of 1-butyl-3-methylimidazolium chloride/cellulosic gel blended with polydiphenylamine. *Sensors and Actuators A: Physical*, *220*, 249–261.

Li, L., Fang, Y., Vreeker, R., & Appelqvist, L. (2007). Reexamining the egg-box model in calcium-alginate gels with X-ray diffraction. *Biomacromolecules*, *8*, 464–468.

Liu, B., & Shaw, T. M. (2001). Electroreology of filled silicone elastomers. *Journal of Rheology*, *45*, 641–657.

Ludeelerd, P., Niamlang, S., Kunaruksapong, R., & Sirivat, A. (2010). Effect of elastomer matrix type on electromechanical response of conductive polypyrrole/elastomer blends. *Journal of Physics and Chemistry of Solids*, *71*, 1243–1250.

Mirfakhrai, T., Madden, D. W., & Baughman, R. H. (2007). Polymer artificial muscles. *Material Today*, *10*, 30–38.

Niamlang, S., & Sirivat, A. (2008). Dielectrophoresis force and deflection of electroactive poly(p-phenylene vinylene)/polydimethylsiloxane blends. *Smart Materials and Structures*, *17*(1–8), 035036

Paradee, N., & Sirivat, A. (2014). Synthesis of poly(3,4-ethylenedioxythiophene) nanoparticles via chemical oxidationpolymerization. *Polymer International*, *63*, 106–113.

Paradee, N., Sirivat, A., Niamlang, S., & Prissanaroon-Ouajai, W. (2012). Effects of crosslinking ratio, model drugs: and electric field strength on electrically controlled release for alginate-based hydrogel. *Journal of Materials Science: Materials in Medicine*, *23*, 999–1010.

Pattavarakorn, D., Youngta, P., Jaesrichai, S., Thongbor, S., & Chaimongkol, P. (2013). Electroactive performances of conductive polythiophene/hydrogel hybrid artificial muscle. *Energy Procedia*, *34*, 673–681.

Petcharoen, K., & Sirivat, A. (2016). Magneto-electro-responsive material based on magnetite nanoparticles/polyurethane composites. *Materials Science and Engineering C: Materials for Biological Applications*, *61*, 312–323.

Petcharone, K., & Sirivat, A. (2013). Electroactive properties of thermoplastic polyurethane elastomer: effects of urethane type and soft-hard segment composition. *Current Applied Physics*, *13*, 1119–1127.

Puvanatvattana, T., Chotpattananont, D., Hiamtup, P., Niamlang, S., Sirivat, A., & Jamieson, A. M. (2006). Electric field induced stress moduli in polythiophene/polyisoprene elastomer blends. *Reactive and Functional Polymers*, *66*, 1575–1588.

Raj, V., Madheswari, D., & Ali, M. M. (2010). Chemical formation: characterization and properties of polycarbazole. *Journal of Applied Polymer Science*, *116*, 147–154.

Saarai, A., Kasparkova, V., Sedlacek, T., & Saha, P. (2013). On the development and characterisation of crosslinked sodium alginate/gelatine hydrogels. *The Mechanical Behavior of Biomedical Materials*, *18*, 152–166.

Sato, T., Watanabe, H., & Osaki, K. (1996). Rheological and dielectric behavior of a styrene-isoprene-styrene triblock copolymer in n-tertradecan. 1. Rubbery-plastic-viscous transition. *Macromolecules*, *29*, 6231–6239.

Srisawasdi, T., Petcharoen, K., & Sirivat, A. (2015). Electromechanical response of silk fibroin hydrogel and conductive polycarbazole/silk fibroin hydrogel composites as actuator material. *Materials Science and Engineering: C*, *56*, 1–8.

Stone, S. A., Gosavi, P., Athauda, T. J., & Ozer, R. R. (2013). In situ citric acid crosslinking of alginate/polyvinyl alcohol electrospun nanofibers. *Materials Letters*, *112*, 32–35.

Tangboriboon, N., Uttanawanit, N., Longtong, M., Wongpinthong, P., Sirivat, A., & Kunanuruksapong, R. (2010). Electrical and electrorheological properties of alumina/natural rubber (STR XL) composites. *Materials*, *3*, 656–671.

Tangboriboon, N., Longtong, M., Sirivat, A., & Kunanuruksapong, R. (2011). Electrical and electromechanical properties of alumina/natural rubber STR 5 L composites. *Materials Technology*, *26*, 100–106.

Tangboriboon, N., Mulsow, L., Kunchornsup, W., & Sirivat, A. (2013). Ceramic granules forming from calcium sodium aluminosilicate and carboxymethyl cellulose. *Journal of Ceramic Processing Research*, *14*, 658–666.

Thipdech, P., Kunanuruksapong, R., & Sirivat, A. (2008). Electromechanical responses of poly(3-thiopheneacetic acid)/acrylonitrile-butadiene rubbers. *Express Polymer Letters*, *2*, 866–877.

Thongsak, K., Kunanuruksapong, R., Sirivat, A., & Lerdwijitjarud, W. (2011). Electroactive polydiphenylamine/poly(styrene-block-isoprene-block-styrene) (SIS) blends: effects of particle concentration and electric field. *Materials Science and Engineering: C*, *31*, 206–214.

Tungkavet, T., Seetapan, N., Pattavarakorn, D., & Sirivat, A. (2012). Improvements of electromechanical properties of gelatin hydrogels by blending with nanowire polypyrrole: effects of electric field and temperature. *Polymer International*, *61*, 825–833.

Voldman, J. (2006). Electrical forces for microscale cell manipulation. *Annual Review of Biomedical Engineering*, *8*, 425–454.

Wang, J., Liu, B., Li, M., & Pan, Y. (2009). Identifying protein complexes from interaction networks based on clique percolation and distance restriction. BioComp 2009, Las Vegas, NV, USA, 13–16 July 2009.

Well, L. A., & Sheardown, H. (2011). Photosensitive controlled release with polyethylene glycol-anthracene modifield alginate. *European Journal of Pharmaceutics and Biopharmaceutics*, *79*, 304–313.

Zhang, N., Liu, H., Kan, H., Nang, X., Long, H., & Zhou, Y. (2014). The preparation of high-adsorption, spherical: hexagonal boron nitride by template method. *Journal Alloys and Compounds*, *613*, 74–79.

Zhuo, Y., Du, C., Li, X., Sun, W., & Ying Chu, Y. (2013). One-step synthesis and photoluminescence properties of polycarbazole spheres and Ag/polycarbazole core/shellcomposites. *European Polymer*, *49*, 1365–1372.

Zingaretti, L., Boscatto, L., Chiacchiera, M., & Silber, J. (2003). Kinetics and mechanism for the reaction of 1-chloro-2,4-dinitrobenzene with n-butylamine and piperidine in AOT/n-hexane/water reverse micelles. *ARKIVOC*, *34*, 189–200.